JASA ARTICLE

Finite-element numerical simulations of seismic attenuation in finely layered rocks

Stefano Picotti,[1,a)] José M. Carcione,[1] Juan E. Santos,[2,b)] Davide Gei,[1] and Fabio Cavallini[1]

[1]*National Institute of Oceanography and Applied Geophysics – OGS, Trieste, Italy*

[2]*School of Earth Sciences and Engineering, Hohai University, Nanjing 211100, China*

ABSTRACT:

P-wave conversion to slow diffusion (Biot) modes at mesoscopic (small-scale) inhomogeneities in porous media is believed to be the most important attenuation mechanisms at seismic frequencies. This study considers three periodic thin layers saturated with gas, oil, and water, respectively, a realistic scenario in hydrocarbon reservoirs, and perform finite-element numerical simulations to obtain the wave velocities and quality factors along the direction perpendicular to layering. The results are validated by comparison to the Norris-Cavallini analytical solution, constituting a cross-check for both theory and numerical simulations. The approach is not restricted to partial saturation but also applies to relevant properties in reservoir geophysics, such as porosity and permeability heterogeneities. This paper considers two cases, namely, the same rock skeleton and different fluids, and the same fluid and different dry-rock properties. Unlike the two-layer case (two fluids), the results show two relaxation peaks and the agreement between numerical and analytical solutions is excellent.

https://doi.org/10.1121/10.0002127

(Received 4 June 2020; revised 11 September 2020; accepted 17 September 2020; published online 13 October 2020)

[Editor: Roel Snieder] Pages: 1978–1983

I. INTRODUCTION

Fluid flow is responsible for the high wave dissipation in partially saturated rocks. Fluid-pressure gradients, induced between regions of dissimilar properties (mesoscopic, small-scale heterogeneities) generate slow P diffusion modes from fast P-waves, according to the Biot theory of poroelasticity, where the mesoscopic scale is much larger than the pore size but much smaller than the wavelength. The mode conversion is very effective in the presence of partial saturation. This dissipation mechanism was first explained by White *et al.* (1975) for a two-layer periodic system and extended by Norris (1993) to many layers. Although these theories consider each layer as a medium saturated with a single fluid, P-waves "see" the layering as a partially saturated medium at the long wavelength limit. Cavallini *et al.* (2017) explicitly solved Norris's equations and obtained a solution for three layers. For example, if the fluid content or the porosity of the rock skeleton vary significantly at the mesoscopic scale, fluid diffusion between different regions generates this loss mechanism, which can be important at seismic frequencies (e.g., Carcione, 2014; Carcione and Picotti, 2006; Santos and Gauzellino, 2017).

The advantage of the three-layer system is that the variations in fluid type, porosity, permeability, and dry-rock bulk moduli can be arbitrary. Periodicity is not a limitation since, according to Norris (1993), the characteristic length defining the periodicity can be the spatial autocorrelation length in a non-periodically (random) layered medium (see Gurevich and Lopatnikov, 1995). In this work, the theory of Norris (1993) and Cavallini *et al.* (2017) is verified by means of a numerical method. To verify the theory [and the finite element (FE) numerical solver], we perform numerical simulations of oscillatory (harmonic) numerical simulations based on a space-frequency domain FE method. We apply the methodology to the periodic sequence of three layers and compute the quality factor and wave velocities as a function of frequency along the direction perpendicular to layering. This methodology has already been used with success in other simpler cases (Carcione, 2014; Carcione *et al.*, 2011; Picotti *et al.*, 2010; Santos *et al.*, 2009).

II. THEORY

Let us consider isotropic poroelastic layers and denote the time variable by t, the frequency by $f = \omega/(2\pi)$, where ω is the angular frequency, and the position vector by $\mathbf{x} = (x, y, z) = (x_1, x_2, x_3)$. Let $u^s(\mathbf{x}) = (u_1^s, u_2^s, u_3^s)$ and $u^f(\mathbf{x}) = (u_1^f, u_2^f, u_3^f)$ indicate the time Fourier transform of the displacement vector of the solid and fluid (relative to the solid) phases, respectively [if U^f is the fluid displacement vector, $u^f = \phi(U^f - u^s)$, where ϕ is the porosity]. Also, set $u = (u^s, u^f)$, let $\sigma_{ij}(u)$ and $p_f(u)$ denote the time Fourier transform of the total stress and the fluid pressure, respectively, and let $\epsilon_{ij}(u^s)$ be the strain tensor of the solid phase.

A. Stress-strain relation

The frequency-domain stress-strain relations of a single plane layer n in a sequence of $n = 1, 2, 3$ layers, are (Carcione, 2014)

a)Electronic mail: spicotti@inogs.it

b)Also at: Universidad de Buenos Aires, Facultad de Ingenieria, Instituto del Gas y del Petróleo, Av. Las Heras 2214, Piso 3, Buenos Aires, Argentina.

$$\sigma_{kl}(u) = 2\mu^{(n)}\,\epsilon_{kl}(u^s) + \delta_{kl}\left(\lambda_G^{(n)}\,\nabla\cdot u^s + \alpha^{(n)}M^{(n)}\nabla\cdot u^f\right), \tag{1}$$

where δ_{kl} is the Kronecker delta and

$$p_f(u) = -\alpha^{(n)}M^{(n)}\nabla\cdot u^s - M^{(n)}\nabla\cdot u^f. \tag{2}$$

For each layer n, the coefficient μ is the shear modulus of the bulk material, considered to be equal to the shear modulus of the dry frame (skeleton). Also

$$\lambda_G = K_G - \frac{2}{3}\mu, \tag{3}$$

with K_G the bulk modulus of the saturated material (Gassmann modulus). The coefficients in Eqs. (1) and (2) can be obtained from the relations (Carcione, 2014)

$$\alpha = 1 - \frac{K_m}{K_s}, \quad M = \left(\frac{\alpha-\phi}{K_s} + \frac{\phi}{K_f}\right)^{-1}, \quad K_G = K_m + \alpha^2 M, \tag{4}$$

where K_s, K_m, and K_f denote the bulk moduli of the solid grains, dry frame, and saturant fluid, respectively. The coefficient α is known as the effective stress coefficient of the bulk material.

B. Equation of motion

We define the matrix

$$\mathcal{B} = \begin{pmatrix} 0I & 0I \\ 0I & bI \end{pmatrix}, \tag{5}$$

which is positive definite and non-negative. Here, I is the 3 $\times$ 3 identity matrix, and the coefficient b includes the viscous coupling effects between the solid and the fluid,

$$b = \frac{\eta}{\kappa}, \tag{6}$$

where η is the fluid viscosity and κ is the frame permeability.

Next, let $\mathcal{L}(u)$ be the second-order differential operator defined by

$$\mathcal{L}(u) = \left[\nabla\cdot\sigma(u), -\nabla p_f(u)\right]^\top. \tag{7}$$

Biot's equation of motion in the diffusive range, stated in the space-frequency domain, is

$$\mathrm{i}\omega\mathcal{B}u(x,\omega) - \mathcal{L}[u(x,\omega)] = 0, \tag{8}$$

which is complemented with Eqs. (1) and (2). We have ignored external sources in Eq. (8) and the inertial (acceleration) term, which can be neglected since over the seismic band of frequencies that term is negligible compared to the viscous resistance. Equation (8) describes wave diffusion in a porous medium and is the basis to take into account the mesoscopic-loss anelasticity introduced by White *et al.* (1975) for two layers and generalized by Norris (1993) to many layers. Therefore, at this frequency band, the effects of wave-induced fluid flow are described by the quasi-static Biot theory, i.e., stress equilibrium within the porous frame and Darcy's flow of pore fluid (e.g., Carcione *et al.*, 2011; Carcione, 2014, Chap. 7; Santos and Gauzellino, 2017, Chap. 7).

The mesoscopic attenuation theory of interlayer flow from White *et al.* (1975), extended by Norris (1993), describes the equivalent viscoelastic medium of a stack of thin alternating porous layers of thickness L_j, $j = 1, 2, 3$, such that the period of the stratification is $L = \sum_j L_j$. The theory gives the complex and frequency dependent P-wave modulus E, where the analytical solution is given in Appendix A.4, specifically Eq. (61), from Cavallini *et al.* (2017). Defining ρ_s and ρ_f as the mass densities of the solid grains and fluid, respectively, the bulk density is

$$\rho = (1-\phi)\rho_s + \phi\rho_f. \tag{9}$$

C. Seismic properties

The P-wave phase velocity is given by

$$v_p = \left[\mathrm{Re}\left(\frac{1}{v}\right)\right]^{-1}, \tag{10}$$

where v is the complex velocity

$$v = \sqrt{\frac{E}{\rho}}, \tag{11}$$

and the quality factor is

$$Q = \frac{\mathrm{Re}(v^2)}{\mathrm{Im}(v^2)}, \tag{12}$$

(e.g., Carcione, 2014). The modulus E is equivalent to the complex stiffness component p_{33} of the effective (long-wavelength) transversely isotropic medium.

D. Peak frequency and diffusion length

The approximate transition frequency separating the relaxed and unrelaxed states (i.e., the approximate location of the relaxation peak) is (Carcione, 2014)

$$f_{0j} = \frac{8\kappa M E_m}{\pi\eta L_j^2 E_G}, \quad j = 1, 2, 3, \tag{13}$$

where M, $E_m = K_m + 4\mu/3$, $E_G = K_G + 4\mu/3$, η, and L_j refer to every single layer. At this reference frequency, the Biot slow-wave attenuation length equals the mean layer thickness or characteristic length of the inhomogeneities (see next paragraph). Equation (13) indicates that the relaxation peak moves towards the low frequencies with increasing viscosity and decreasing permeability, i.e., the opposite behaviour of the Biot peak.

The dissipation is due to the presence of the slow P-wave, with a diffusivity constant $d = \kappa M E_m/(\eta E_G)$, while the critical fluid-diffusion relaxation length is $L_r = \sqrt{d/\omega}$. The fluid pressures will be equilibrated if L_r is comparable to the period of the stratification. For smaller diffusion lengths (e.g., higher frequencies) there is not enough time for the pressures to reach equilibrium, causing attenuation and velocity dispersion. Since $\omega = 2\pi f$ and $f = d/(2\pi L_r^2)$, substituting the diffusivity constant d into this equation, we have that the transition frequency [Eq. (13)] is obtained for a diffusion length $L_r = L_j/4$ (Carcione, 2014).

III. HARMONIC NUMERICAL SIMULATIONS

We perform harmonic numerical simulations to compute the stiffness E as a function of frequency by using a Galerkin FE procedure (Carcione *et al.*, 2011; Santos *et al.*, 2009). A square sample Ω of boundary Γ of the periodic 3-layer medium is subjected to time-harmonic compressions $\Delta P \exp(\mathrm{i}\omega t)$, where P denotes pressure (see Fig. 1) and Δ denotes a variation of the field variable. In the following, we establish the boundary conditions to be used at the sides of Ω to obtain the stiffness components. Then, we solve Eq. (8) with those conditions.

The boundary of Ω is $\Gamma = \Gamma^L \cup \Gamma^B \cup \Gamma^R \cup \Gamma^T$, where

$$\Gamma^L = \{(x,z) \in \Gamma : x = 0\}, \quad \Gamma^R = \{(x,z) \in \Gamma : x = D\},$$
$$\Gamma^B = \{(x,z) \in \Gamma : z = 0\}, \quad \Gamma^T = \{(x,z) \in \Gamma : z = D\}, \tag{14}$$

where D is the side length of Ω, Γ^L, Γ^R, Γ^B, and Γ^T are the left, right, bottom, and top boundaries of Ω, respectively. Denote by $\mathbf{n}$ the unit outer normal on Γ and let $\mathbf{m}$ be a unit tangent on Γ so that $\{\mathbf{n}, \mathbf{m}\}$ is an orthonormal system on Γ. The boundary conditions are

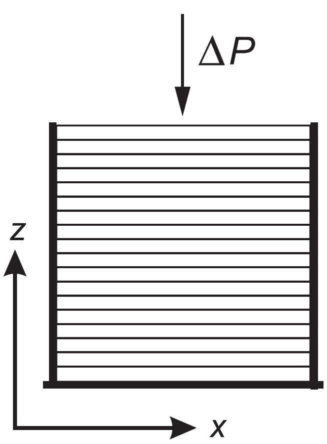

FIG. 1. Oscillatory (harmonic) test performed to obtain E. The orientation of the layers and the directions of the applied stress are indicated. The thick black lines at the edges indicate rigid boundary conditions (vanishing normal solid and fluid displacements and tangential stresses).

$$(\sigma \mathbf{n}) \cdot \mathbf{n} = -\Delta P, \quad (x,z) \in \Gamma^T,$$
$$(\sigma \mathbf{n}) \cdot \mathbf{m} = 0, \quad (x,z) \in \Gamma,$$
$$u \cdot \mathbf{n} = 0, \quad (x,z) \in \Gamma^L \cup \Gamma^R \cup \Gamma^B. \tag{15}$$

Only the strain component ϵ_{33} is non-zero, while $\epsilon_{11} = \epsilon_{22} = 0$. Denoting by V the original volume of the sample and by $\Delta V(\omega)$ its (complex) oscillatory volume change, we have

$$\frac{\Delta V(\omega)}{V} = -\frac{\Delta P}{E(\omega)}, \tag{16}$$

valid in the quasi-static case. After solving Eq. (8) with the boundary conditions [Eq. (15)], we obtain the average vertical displacement $u_3^T(\omega)$ at the top boundary Γ^T from the vertical displacements $u_3(x, D, \omega)$ measured on Γ^T. Then, for each frequency ω, the volume change produced by the compressibility test can be approximated by $\Delta V(\omega) \approx L u_3^T(\omega)$, which yields $E(\omega)$ using the relation [Eq. (16)].

To estimate $E(\omega)$, we use a FE procedure to compute the solution of the equations of motion [Eq. (8)], based on bilinear functions to represent the solid displacement vector, whereas the fluid displacement is approximated by a closed subspace of the vector part of the Raviart–Thomas–Nedelec space of zero order (Raviart and Thomas, 1977; Nedelec, 1980). More details about this methodology can be found in (Carcione, 2014, Chap. 4; Santos and Gauzellino, 2017, Chap. 6; Santos *et al.*, 2009). Finally, we obtain the P-wave velocity and quality factor using equations (10) and (12).

IV. EXAMPLES

We consider two examples, where the inhomogeneities are due to the pore fluids and the frame, respectively. To obtain a reliable comparison between the Norris-Cavallini theory and the numerical solution, the model should include a large number of periods, which requires a large mesh, with a consequent increase in the amount of storage and computer time. Therefore, the choice of the mesh size is a compromise between the computational effort and solution reliability. The sample model, represented in Fig. 1, is discretized on a numerical mesh of 210 $\times$ 210 grid points. Each example considers five cases with a grid spacing of 4 cm, except case 5, which uses 2 cm. A smaller grid spacing is used for case 5 to discretize a very thin layer (at least two points per layer thickness are needed). As a result, the number of periods is 14 for all the cases and seven for case 5.

A. Homogenous frame example

The first example considers the same frame (skeleton) and three thin layers of period $L = 60$ cm saturated with brine, oil, and gas, where the properties of the rock, frame, and saturant fluids are listed in Table I.

The thicknesses are denoted by $L_i = LS_i$, where S_i represents the saturations, denoted by S_b, S_o, and S_g for brine, oil, and gas, respectively. Figure 2 shows the phase velocity

TABLE I. Medium properties.

Grain	Bulk modulus, K_s	33.4 GPa
	Shear modulus, μ_s	30 GPa
	Density, ρ_s	2650 kg/m^3
Frame	Bulk modulus, K_m	1.3 GPa
	Shear modulus, μ_m	1.4 GPa
	Porosity, ϕ	0.3
	Permeability, κ	1 darcy
Brine	Density, ρ_B	975 kg/m^3
	Viscosity, η_B	0.001 Pa s
	Bulk modulus, K_B	2.2 GPa
Oil	Density, ρ_o	870 kg/m^3
	Viscosity, η_o	0.3 Pa s
	Bulk modulus, K_o	2 GPa
Gas	Density, ρ_g	70 kg/m^3
	Viscosity, η_g	0.00015 Pa s
	Bulk modulus, K_g	0.0096 GPa

[Fig. 2(a)] and dissipation factor (inverse of the quality factor) [Fig. 2(b)] for each case indicated in Table II, where the symbols correspond to the FE solution. As can be observed, the agreement between the solutions is very good.

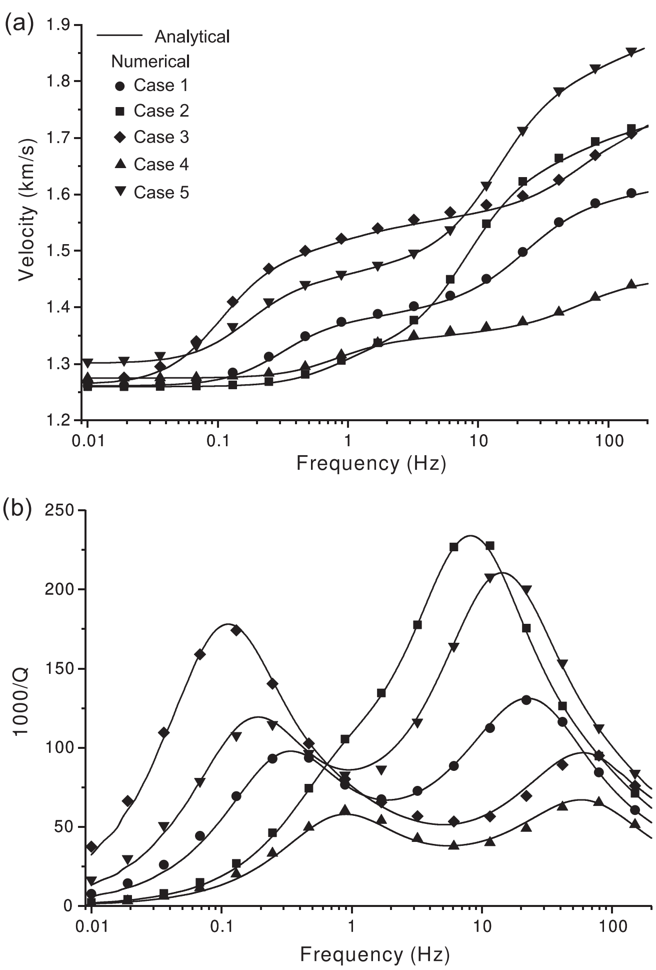

FIG. 2. P-wave phase velocity (a) and dissipation factor (b) corresponding to the cases shown in Table II. The symbols refer to the FE numerical simulations.

TABLE II. Homogeneous frame. Saturations of brine, oil, and gas.

Case	S_b (%)	S_o (%)	S_g (%)
1	100/3	100/3	100/3
2	60	20	20
3	20	60	20
4	20	20	60
5	46.7	46.7	6.6

Unlike the second case (where brine has the highest saturation) the other curves show two attenuation peaks. Based on the approximated transition frequency [Eq. (13)], the lower- and higher-frequency dissipation peaks are related to the presence of oil and gas, respectively. For example, in case 3 we have $f_{02} = 0.14$ Hz and $f_{03} = 37.4$ Hz, while the first peak has a negligible amplitude and is located at a very high frequency. When the transition frequencies are similar, we have one peak as in case 2, where $f_{01} = 43.9$ Hz, $f_{02} = 1.28$ Hz, and $f_{03} = 37.4$ Hz. The peak amplitudes in these examples indicate high attenuation, with minimum quality factors between 5 and 20. To our knowledge, the use of attenuation in surface seismics for reservoir characterization has been very limited. P-wave quality factors computed from field data in sandstone reservoirs (e.g., Klimentos, 1995) show that attenuation can be very strong at sonic frequencies ($5 < Q < 30$). Assuming that similar pore-fluid effects occur at seismic frequencies, these simulations predict that attenuation can be important for seismic data as well, allowing us to distinguish between different proportions of gas, oil, and water.

B. Homogeneous fluid example

The second example considers three layers of dissimilar porosity saturated with brine. Porosity and permeability are related by the Kozeny-Carman relation (Mavko *et al.*, 2009),

$$\kappa = \frac{4B\phi^3 R^2}{(1-\phi)^2}, \tag{17}$$

where R is the grain radius, $B = 0.003$, and $R = 80$ μm. We use the Krief model (Mavko *et al.*, 2009) to obtain the dry-rock moduli as

$$K_m = K_s(1-\phi)^{3/(1-\phi)} \quad \text{and} \quad \mu = K_m\mu_s/K_s, \tag{18}$$

where μ_s is the shear modulus of the grains. Table III shows the five cases with different layer thicknesses.

The porosities, dry-rock moduli, and permeabilities are given at the bottom of Table III and the other remaining properties are listed in Table I. Figure 3 shows the phase velocity [Fig. 3(a)] and dissipation factor [Fig. 3(b)], respectively, where the symbols correspond to the FE solution. As can be seen, the agreement between the solutions is very good. Compared to the homogeneous frame, there is a

TABLE III. Heterogeneous frame, brine saturated. Layer thicknesses and dry-rock properties.

Case	L_1 (cm)	L_2 (cm)	L_3 (cm)
1	20	20	20
2	36	12	12
3	12	36	12
4	12	12	36
5	4	28	28
ϕ (%)	30	20	10
K_m (GPa)	7.2	14.5	23.5
μ_m (GPa)	6.5	13	21.1
κ (darcy)	1	0.24	0.02

single, relevant attenuation peak with lower amplitude (i.e., lower attenuation), and relaxation frequency between 7 and 100 Hz. Minor peaks at very high transition frequencies are not visible. As for the homogeneous frame, in some cases (e.g., cases 3 and 5) the main broad peak is the superposition of two peaks with similar transition frequencies. For example, using Eq. (13) for case 5, we obtain $f_{02} = 73.6$ Hz and $f_{03} = 13$ Hz.

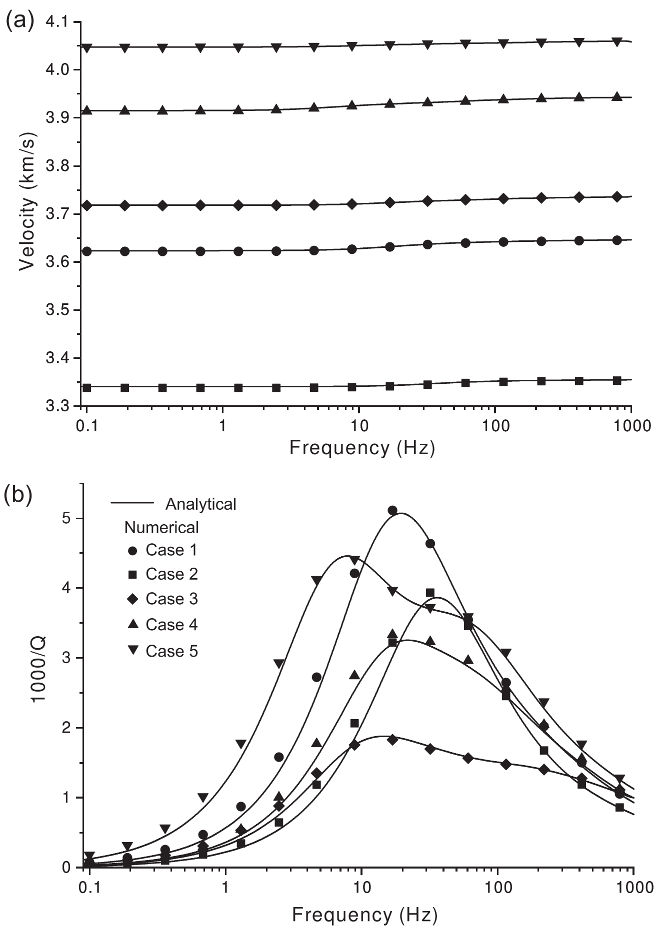

FIG. 3. P-wave phase velocity (a) and dissipation factor (b) corresponding to the cases shown in Table III. The symbols refer to the FE numerical simulations.

V. CONCLUSIONS

Fluid type (bulk modulus, viscosity), permeability, and porosity may, in principle, be inferred from the amplitude and phase of the seismic pulse, related to the quality factor and phase velocity, respectively. We have presented numerical quasi-static harmonic numerical simulations to test and validate the theory. The proposed numerical simulations are based on a FE solution of the equation of motion in the space-frequency domain to simulate compressibility tests and obtain the P-wave modulus. We considered three plane layers with different properties and have explicitly obtained the P-wave velocity and quality factor perpendicular to layering. The first example considers the same skeleton saturated with brine, oil, and gas. The curves show two attenuation peaks, unlike the case of two fluids. A second example assumes three layers of different porosity saturated with brine. The agreement with the analytical solution is excellent in both cases.

The FE numerical simulations are not restricted to obtain the properties perpendicular to layering but can be used to obtain the five stiffness components of the equivalent transversely-isotropic medium. In future work, we will extend the computation to the anisotropic case. Because the fluid flow is perpendicular to the layering plane, there is only one relaxation function, corresponding to the symmetry-axis P-wave stiffness. Knowing this relaxation function and the high- and low-frequency elastic limits of the stiffness tensor, the seismic properties as a function of the propagation angle can be obtained.

Carcione, J. M. (**2014**). *Handbook of Geophysical Exploration Wave Fields in Real Media: Wave Propagation in Anisotropic, Anelastic, Porous and Electromagnetic Media*, 3rd ed. (Elsevier Science, Amsterdam, the Netherlands).

Carcione, J. M., and Picotti, S. (**2006**). "P wave seismic attenuation by slow-wave diffusion: Effects of inhomogeneous rock properties," Geophysics **71**, 1–8.

Carcione, J. M., Santos, J. E., and Picotti, S. (**2011**). "Anisotropic poroelasticity and wave-induced fluid flow. Harmonic finite-element simulations," Geophys. J. Internat. **186**, 1245–1254.

Cavallini, F., Carcione, J. M., de Ventos, D. V., and Engell-Sørensen, L. (**2017**). "Low-frequency dispersion and attenuation in anisotropic partially saturated rocks," Geophys. J. Internat. **209**(3), 1572–1584.

Gurevich, B., and Lopatnikov, S. (**1995**). "Velocity and attenuation of elastic waves in finely layered porous rocks," Geophys. J. Int. **121**, 933–947.

Klimentos, T. (**1995**). "Attenuation of P- and S-waves as a method of distinguishing gas and condensate from oil and water," Geophysics **60**(2), 447–458.

Mavko, G., Mukerji, T., and Dvorkin, J. (**2009**). *The Rock Physics Handbook: Tools for Seismic Analysis of Porous Media* (Cambridge University Press, Cambridge, UK).

Nedelec, J. C. (**1980**). "Mixed finite elements in R^3," Numer. Math. **35**, 315–341.

Norris, A. N. (**1993**). "Low-frequency dispersion and attenuation in partially saturated rocks," J. Acoust. Soc. Am. **94**, 359–370.

Picotti, S., Carcione, J. M., Santos, J. E., and Gei, D. (**2010**). "Q-anisotropy in finely layered media," Geophys. Res. Lett. **37**, L06302, https://doi.org/10.1029/2009GL042046.

Raviart, P., and Thomas, J. M. (**1977**). "Mixed finite element method for 2nd order elliptic problems," in *Mathematical Aspects of the Finite Element Methods*, edited by I. Galligani and E. Magenes (Springer-Verlag, New York), pp. 292–315.

Santos, J. E., and Gauzellino, P. M. (**2017**). *Lecture Notes in Geosystems Mathematics and Computing Numerical Simulation in Applied Geophysics* (Birkhauser, Springer, New York).

Santos, J. E., Rubino, J. G., and Ravazolli, C. L. (**2009**). "A numerical upscaling procedure to estimate effective plane wave and shear moduli in heterogeneous fluid-saturated poroelastic media," Comput. Methods Appl. Mech. Eng. **198**, 2067–2077.

White, J. E., Mikhaylova, N. G., and Lyakhovitskiy, F. M. (**1975**). "Low-frequency seismic waves in fluid saturated layered rocks," Izvestija Acad. Sci. USSR. Phys. Solid Earth **11**, 654–659.